Selectivity for the rate of frequency-modulated sweeps in the mouse auditory cortex

Michael Trujillo, Kevin Measor, Maria Magdalena Carrasco and Khaleel A. Razak

J Neurophysiol 106:2825-2837, 2011. First published 17 August 2011; doi:10.1152/jn.00480.2011

J Neurophysiol 106: 2825–2837, 2011.
First published August 17, 2011; doi:10.1152/jn.00480.2011.

Selectivity for the rate of frequency-modulated sweeps in the mouse auditory cortex

Michael Trujillo,[1] Kevin Measor,[1] Maria Magdalena Carrasco,[1] and Khaleel A. Razak[2]
[1]*Graduate Neuroscience Program and* [2]*Department of Psychology, University of California, Riverside, California*

Submitted 31 May 2011; accepted in final form 16 August 2011

Trujillo M, Measor K, Carrasco MM, Razak KA. Selectivity for the rate of frequency-modulated sweeps in the mouse auditory cortex. *J Neurophysiol* 106: 2825–2837, 2011. First published August 17, 2011; doi:10.1152/jn.00480.2011.—Frequency-modulated (FM) sweeps are common components of vocalizations, including human speech. Both sweep direction and rate influence discrimination of vocalizations. Across species, relatively less is known about FM rate selectivity compared with direction selectivity. In this study, FM rate selectivity was studied in the auditory cortex of anesthetized 1- to 3-mo-old C57bl/6 mice. Neurons were classified as fast pass, band pass, slow pass, or all pass depending on their selectivity for rates between 0.08 and 20 kHz/ms. Multiunit recordings were used to map FM rate selectivity at depths between 250 and 450 μm across both primary auditory cortex (A1) and the anterior auditory field (AAF). In terms of functional organization of rate selectivity, three patterns were found. First, in both A1 and AAF, neurons clustered according to rate selectivity. Second, most (~60%) AAF neurons were either fast-pass or band-pass selective. Most A1 neurons (~72%) were slow-pass selective. This distribution supports the hypothesis that AAF is specialized for faster temporal processing than A1. Single-unit recordings (n = 223) from A1 and AAF show that the mouse auditory cortex is best poised to detect and discriminate a narrow range of sweep rates between 0.5 and 3 kHz/ms. Third, based on recordings obtained at different depths, neurons in the infragranular layers were less rate selective than neurons in the granular layers, suggesting FM processing undergoes changes within the cortical column. On average, there was very little direction selectivity in the mouse auditory cortex. There was also no correlation between characteristic frequency and direction selectivity. The narrow range of rate selectivity in the mouse cortex indicates that FM rate processing is a useful physiological marker for studying contributions of genetic and environmental factors in auditory system development, aging, and disease.

speed tuning; columnar organization; cortical areas; vocal processing

FREQUENCY-MODULATED (FM) sweeps are common components of animal vocalizations, including human speech. FM sweeps are important in discrimination of speech sounds (Stevens and Klatt 1974; Zeng et al. 2005). Deficits in spectrotemporal processing can lead to speech perception impairments, and cognitive training programs that utilize FM sweeps can alleviate some of these impairments (Merzenich et al. 1996; Smith et al. 2009; Tallal and Piercy 1973). Presbycusis, or normal aging-related decline in speech processing, may be related to a difficulty in processing rapid formant transitions present in consonants. This suggests that deficits in following frequency transitions may cause speech processing decline (Gordon-Salant and Fitzgibbons 2001). The auditory cortex of all species examined contains neurons sensitive to the rate and direction of FM sweeps (Atencio et al. 2007; Brown and Harrison 2009; Godey et al. 2005; Heil et al. 1992; Nelken and Versnel 2000; Razak and Fuzessery 2006; Suga 1965; Tian and Rauschecker 1994; Tian and Rauschecker 2004; Washington and Kanwal 2008). Furthermore, the mechanisms of FM sweep selectivity have been characterized in the auditory system (Fuzessery et al. 2006; Gittelman et al. 2009; Gittelman and Pollak 2011; Gordon and O'Neill 1998; Razak and Fuzessery 2006, 2008, 2009; Ye et al. 2010). Collectively, these studies suggest that an analysis of FM sweep processing is a useful step in understanding representations of species-specific vocalizations.

The genetic engineering tools currently available make the mouse nervous system a suitable model to study neural dysfunctions caused by genetic disorders and to probe underlying mechanisms. In auditory system research, the mouse holds significant promise in elucidating the mechanisms underlying vocal communication disorders. To provide the foundation for investigating mechanisms of auditory processing dysfunctions, particularly in relation to spectrotemporally complex sounds, the main objective of this study was to determine selectivity for FM sweeps in the auditory cortex of the mouse.

FM sweep selectivity has been studied in the mouse inferior colliculus (Hage and Ehret 2003), but not in the auditory cortex. A comparison of the two areas will provide information on how the representation of spectrotemporally dynamic sounds changes within the ascending auditory system. In mice and across species, relatively less is known about FM sweep rate selectivity compared with direction selectivity. Therefore the first goal of this study was to map FM rate selectivity in both primary auditory cortex (A1) and anterior auditory field (AAF) using a broad range of frequency sweep rates in the mouse (C57bl/6 strain) auditory cortex. A1 and AAF were compared with test the hypothesis that the AAF is more specialized for faster temporal processing (Linden et al. 2003). Recent studies in the cat auditory cortex suggest that neurons in deeper cortical layers are less selective for stimulus features compared with the granular input layers, suggesting hierarchical processing within the cortical column (Atencio et al. 2009; Atencio and Schreiner 2010). The second aim of this study was to determine whether there are cortical depth-specific differences in FM rate selectivity in the mouse auditory cortex. The C57 strain of mice was chosen because it forms the background for various knockout strains used as disease models. The data in this study can therefore serve as control for future investigations of FM sweep processing in transgenic mice.

Address for reprint requests and other correspondence: K. Razak, Dept. of Psychology, 900 Univ. Ave., Univ. of California, Riverside, CA 92521 (e-mail: khaleel@ucr.edu).

METHODS

The Institutional Animal Care and Use Committee at the University of California, Riverside approved all procedures. Mice (C57bl/6 strain) were obtained from an in-house breeding colony that originated from breeding pairs purchased from Jackson Laboratory (Bar Harbor, ME). Mice were housed with 2–5 littermates under a 15:9-h light-dark cycle and fed ad libitum. These mice were studied before the onset of accelerated hearing loss (age <3 mo).

Surgical procedures. Mice were anesthetized with an intraperitoneal injection of ketamine (150 mg/kg) and xylazine (10 mg/kg) mixture and maintained throughout the experiment via either supplemental dosing with ketamine-xylazine or isoflurane inhalation (0.2–0.5% in air). Anesthetic state was monitored throughout the experiment using the toe-pinch reflex test, and supplemental anesthetic was administered or isoflurane concentration was increased as needed. Once an areflexic state of anesthesia was reached, measured by a toe pinch, a scalp incision was made along the midline and the right temporalis muscle was reflexed. The skull was cleaned, and then a craniotomy was performed using a dental drill. The auditory cortex was exposed based on skull and vascular landmarks identified by Willot et al. (1993). Mice were euthanized at the end of the experimental day via an overdose of pentobarbital sodium (125 mg/kg).

Acoustic stimulation. Acoustic stimulation and data acquisition were driven by custom-written software (Batlab; developed by Dr. Don Gans, Kent State University, Kent, OH) and a Microstar digital signal processing board. Programmable attenuators (PA5; Tucker-Davis Technologies, Gainesville, FL) allowed control of sound intensities before amplification by a stereo power amplifier (Parasound HCA1100) or an integrated amplifier (Yamaha AX430). Sounds were delivered through a free-field speaker (LCY-K100 ribbon tweeters; Madisound, Middleton, WI) located 6 in. and 45° from the left ear, contralateral to physiological recordings. Frequency response of the sound delivery system was measured using a ¼-in. Bruel and Kjaer microphone and measuring amplifier and was found to be flat within ± 3 dB for frequencies between 7 and 40 kHz. Frequencies 5 kHz and below were filtered out (Butterworth, 24 dB/octave, Krohn-Hite).

Electrophysiology. Mice were placed in a stereotaxic apparatus (model 930; Kopf, Tujunga, CA) and secured in a mouse bite bar adapter (model 923B; Kopf). Experiments were conducted in a heated (~80°F), sound-attenuated chamber lined with anechoic foam (Gretch-Ken Industries, Lakeview, OR). Electrophysiological recordings were obtained with glass electrodes filled with 1 M NaCl (impedance 2–10 MΩ). Electrodes were driven orthogonally into the cortex (with a Kopf direct drive 2660 micropositioner). For mapping studies, multiunit recordings were obtained between 250 and 450 μm. For response-selectivity studies, single-unit recordings were obtained between depths of 100 and 700 μm. For depth measurements, the zero point was marked when the electrode first touched the surface of the cortex (determined by changes in recording trace and audio monitor output). The consistency of the zero point was also verified when the electrode was pulled out from a penetration. Single-unit recordings were identified by the constancy of amplitude and waveform displayed on an oscilloscope programmed into the data acquisition software. Poststimulus time histograms (PSTHs) were obtained relative to stimulus onset. Action potentials that occurred within 300 ms of stimulus onset were included in the PSTHs. The number of spikes that were elicited over 20 stimulus repetitions was used for quantification.

Data acquisition. The primary auditory cortex of the C57 mouse can be identified via vascular landmarks (Willot et al. 1993) and by increasing characteristic frequencies (CF) in a caudal to rostral direction (Stiebler et al. 1997). The AAF is located immediately rostral to A1 and exhibits a CF reversal relative to A1. The focus of this study was to map A1 and AAF. Other areas such as AII and ultrasonic field, although also present in young C57 mice (Bandyopadhyay et al. 2010; Willot et al. 1993), were not sampled. The excitatory tuning curve was determined by presenting pure tones varying in frequency and intensity. The tone duration used was optimized to maximize response to tones as neurons showed duration selectivity (Brand et al. 2000; Razak K, unpublished observations). The range of durations used was between 2 and 50 ms (rise/fall time 1 ms). The CF was defined as the frequency at which spikes were generated for at least five successive stimulus presentations at the lowest intensity (threshold). The excitatory tuning curve was determined by stepping frequency up and down between 5 and 50 kHz until no response was observed. After the low- and high-frequency edge at a given intensity was determined, intensity was decreased in 10-dB steps and the procedure repeated until threshold and CF were determined.

FM rate selectivity. The first step in determining rate selectivity was to present an FM sweep of fixed bandwidth at different durations. The sweep rate (in kHz/ms) of the stimulus was obtained by dividing the FM bandwidth (in kHz) by the duration (in ms). It is important to present sweeps that not only stimulate the excitatory frequencies but also extend beyond the edges of the tuning curve, because rate selectivity is at least partially shaped by inhibitory sidebands (Razak and Fuzessery 2006). Rate selectivity of a neuron will be different for sweeps that include the sideband compared with sweeps that do not (Razak and Fuzessery 2006). Therefore, FM sweep bandwidths were adapted according to the CF and tuning width. Once the excitatory tuning curve was obtained, linear FM sweeps centered approximately at CF were presented at 10–20 dB above threshold. The sweep bandwidths exceeded the bandwidth of the tuning curve at that intensity by at least 5 kHz. More typically, the sweeps extended outside the tuning curve by at least 10 kHz. Data from the pallid bat auditory cortex (Razak and Fuzessery 2006) and unpublished data from the C57 mouse cortex show that inhibitory sidebands, if present, typically abut the edges of the excitatory tuning curve. Thus our procedure of extending the sweeps outside the tuning curve will capture at least a part of the putative sidebands. FM rates between 0.08 and 20 kHz/ms were tested. These sweep rates were generated using bandwidths between 15 kHz (e.g., 20→5 kHz sweep) and 60 kHz (e.g., 65→5 kHz sweep) and durations between 3 and 200 ms.

Neurons were classified as all pass (AP), band pass (BP), fast pass (FP), or slow pass (SP) according to FM rate selectivity (Felsheim and Ostwald 1996; Mendelson et al. 1993; Poon et al. 1991; Razak and Fuzessery 2006; Ricketts et al. 1998; Tian and Rauschecker 1994). It must be noted that this classification applies to the range of FM rates (0.08–20 kHz/ms) tested in this study. The classification may change if other ranges of FM rates were used. AP neurons responded within 50% of maximum response at all rates tested. BP neurons were selective for a range of rates, with responses decreasing below 50% of maximum for slower and faster rates. FP neurons' responses decreased below 50% of maximum as rates were decreased. SP neurons' responses decreased below 50% of maximum as FM rates were increased.

The 50% cutoff rate, defined as the FM rate at which the response declines to 50% of maximum response, was measured for FP and BP neurons. For BP neurons, two such rates exist. Only the 50% cutoff for decreasing rate was quantified in this study. For BP neurons, the best rate (BR) was determined as the sum of the product of the number of spikes elicited by each FM sweep rate divided by the total spikes elicited by all FM sweep rates (Atencio et al. 2007; Brown and Harris 2009):

$$\mathrm{BR} = \sum(\mathrm{spikes} \times \mathrm{FM\ rate}) / \sum(\mathrm{spikes})$$

To quantify the degree of rate selectivity, the rate tuning index (RTI) was calculated for each neuron as follows:

$$\mathrm{RTI} = (n/n-1) \times [1 - (\mathrm{mean}/\mathrm{max})]$$

where n is the number of FM sweep rates assessed, mean is the average response across all rates tested, and max is the maximum response. This measure is called "speed tuning" in the literature (Atencio et al. 2007; Brown and Harris 2009).

FM direction selectivity. To assess a preference for upward or downward FM sweeps of the same bandwidths and rates, a direction selectivity index (DSI) was calculated as follows:

$$\mathrm{DSI} = (D - U)/(D + U)$$

where D and U are the trapezoidal area under the curve for downward and upward FM sweeps, respectively (modified from O'Neill and Brimijoin 2002; Razak and Fuzessery 2006). DSI values near 1 indicate a preference for downward frequency modulation, and values near −1 indicate preferences for upward frequency modulation. DSI was assessed at three different ranges of FM rate: 0.1–1, 1.1–3, and 3.1–10 kHz/ms.

RESULTS

Single-unit recordings: classification of FM rate selectivity. FM rate selectivity was determined in 223 neurons in both A1 and AAF with CF between 7 and 35 kHz. In 90 of these neurons, rate selectivity was studied using both upward and downward sweeps. In the remaining neurons, only downward sweeps were used. FM rate selectivity was determined by first measuring FM duration selectivity with sweeps of a fixed bandwidth and differing durations. In 102/223 neurons, FM duration selectivity was measured with at least two different FM bandwidths. Multiple FM bandwidth tests facilitate differentiating between FM rate selectivity and sound duration/bandwidth tuning (Razak and Fuzessery 2006; Fuzessery et al. 2006). Figure 1, *A*, *C*, and *E*, shows examples of FM duration selectivity in which two different sweep bandwidths were tested. Note that the selectivity changes with FM bandwidth. When FM sweep rates (in kHz/ms) were calculated by dividing the FM bandwidth by duration and the responses were replotted against FM sweep rate (Fig. 1, *B*, *D*, and *F*), it can be seen that the neuron's rate selectivity is similar regardless of the sweep bandwidth. This indicates that the neuron was indeed selective for FM sweep rates, and not the duration/bandwidth of the sound used.

Figure 1*G* shows the 50% cutoff rates for FP, BP, and SP neurons obtained with a narrow bandwidth and broad bandwidth sweep. In the vast majority (87/102, 85%) of these neurons, the 50% cutoff was within 1 kHz/ms of each other for the two bandwidths. This suggests that these neurons were selective for sweep rate, and not tuned to the sound duration/bandwidth.

Figure 1, *C* and *D*, also addresses another important methodological issue in studying FM sweep selectivity. Short-duration sweeps (<10 ms) were used to generate rapid FM rates. Such short-duration sweeps may appear as clicks and not really test FM processing. However, Fig. 1*C* shows that the neuron can distinguish a 3-ms sweep with a 45-kHz bandwidth (50→5 kHz sweep) and a 3-ms sweep with a 15-kHz (20→5 kHz sweep). The important parameter for this neuron's response was FM rate. The fact that it responded better to a 7-kHz/ms sweep than to the faster 10-kHz/ms sweep also precludes the possibility that these sounds were processed as clicks because of the rapid rates used.

Figure 2 shows examples of the four types of FM rate selectivity (AP, BP, FP, and SP) along with sample PSTHs. The FM rate tuning type was similar regardless of whether total number of spikes or peak firing rate was used to calculate response magnitude in 70% of AP, 82% of BP, 89% of FP, and 78% of SP neurons. In all subsequent analyses, response magnitude was measured as the number of spikes.

Mouse cortical neurons are selective for a narrow range of FM rates. FM-selective neurons in A1 and AAF exhibit a narrow range of selectivity for FM sweep rates (Fig. 3, *A–D*). The narrow range of selectivity was striking given that a broad range of FM sweep rates (0.08–20 kHz/ms) were tested. For FP neurons (Fig. 3*A*), ~70% of neurons had a 50% cutoff rate between 0.5 and 2 kHz/ms for both upward (11/16 neurons) and downward sweeps (23/33 neurons). For SP neurons (Fig. 3*B*), the 50% cutoff of the majority of neurons was between 0.5 and 2 kHz/ms. No difference was observed between upward and downward sweep 50% cutoff rates for FP and SP neurons (1-way ANOVA, $P = 0.17$).

BP neurons were selective for a narrow range of FM sweep rates. BP neurons had two different 50% cutoff rates, one as sweep rate was decreased (Fig. 3*C*) and one as sweep rate was increased (Fig. 3*D*). The 50% cutoff rate-slow was between 0.5 and 2 kHz/ms in 74% (31/42) of neurons tested with upward sweeps and in 87% (76/87) of neurons tested with downward sweeps. No difference was observed between upward and downward sweep 50% cutoff rates for BP neurons. The 50% cutoff rate-fast (Fig. 3*D*) was more evenly distributed across the rates tested, with ~80% of neurons exhibiting cutoff rates <12 kHz/ms. The best rate of BP neurons also showed a narrow range with best rates between 1 and 3 kHz/ms in 47% of neurons tested with upward sweeps and in 71% of neurons tested with downward sweeps (Fig. 3*E*). Almost all BP neurons tested had best rates between 1 and 7 kHz/ms. These data show that the vast majority of FP neurons will respond best for FM rates faster than ~1–2 kHz/ms and that the sweep rates over which maximum firing rate change occurs in FP neurons is ~1 kHz/ms. Likewise, the majority of SP neurons will respond best to rates slower than ~1–2 kHz/ms, and the maximal change in their firing rate occurs for rates ~1–2 kHz/ms. The majority of BP cells will respond best to rates ~1–4 kHz/ms.

Rate tuning index (RTI) is a quantitative measure that shows the degree to which a neuron is selective for a given FM sweep rate (Atencio et al. 2007; Brown and Harris 2009). The RTI is useful in making comparisons of rate selectivity across species. Table 1 shows the mean (±SE) RTI for the different types of neurons and for the two sweep directions. As expected, the AP neurons had the lowest average RTI.

Effect of anesthetic type. In the presentation above, data obtained from mice anesthetized with ketamine-xylazine for both induction and maintenance (KX) were combined with data from ketamine-xylazine for induction and isoflurane for maintenance (KXI). The justification for combining data was that no differences were found between the two anesthetic groups in terms of 50% cutoff for FP neurons ($n = 25$ with KX, $n = 8$ with KXI; t-test, $P = 0.75$) or RTI ($P = 0.64$). Likewise, for BP neurons ($n = 76$ with KX, $n = 11$ with KXI), no difference was found for 50% cutoff rate (t-test, $P = 0.71$), RTI ($P = 0.32$), or best rate ($P = 0.71$).

Comparison of cortical data from 1- to 2-mo-old mice with data from 2- to 3-mo-old mice. The C57 strain undergoes early onset presbycusis, with high-frequency hearing loss starting at ~3 mo. Cochlear function and auditory responses in the C57 strain are comparable to the CBA strain at ~2 mo of age. We

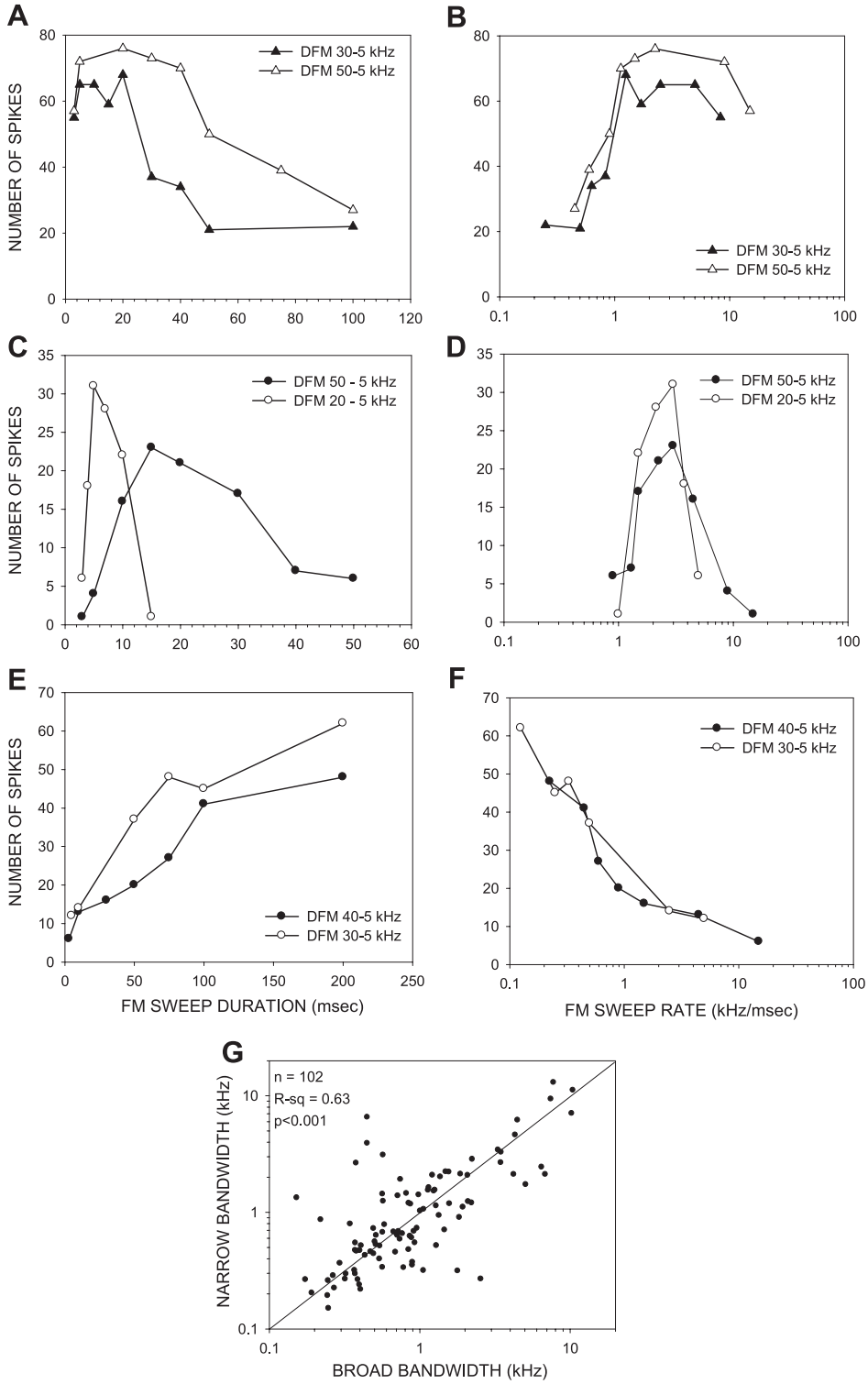

Fig. 1. Rate selectivity functions (*B*, *D*, *F*) were plotted from duration selectivity functions (*A*, *C*, *E*) wherein the bandwidth of the frequency-modulated (FM) sweep (in kHz) is divided by the duration of the FM sweep (in ms) to obtain the FM sweep rate in kHz/ms. These neurons were not selective for sound duration or bandwidth, but they were selective for FM rate. DFM, downward FM sweep. *G*: scatter plot of the 50% cutoff at multiple bandwidths for band-pass (BP), fast-pass (FP), and slow-pass (SP) neurons. The *x*-axis represents the 50% cutoff for broad-bandwidth FM sweeps. The *y*-axis represents the 50% cutoff for narrow bandwidths. The diagonal line represents equal 50% cutoff rates for the 2 different bandwidths used.

compared rate selectivity between 1- to 2-mo-old (30–60 days) and 2- to 3-mo-old mice (61–89 days) to determine whether there are differences that may suggest abnormal processing in the latter group. A *t*-test between the two age groups of RTI showed no difference in BP ($t = 1.69$, $P > 0.05$), FP ($t = -1.45$, $P > 0.05$), and SP neurons ($t = -0.99$, $P > 0.05$). A *t*-test between the age groups of 50% cutoff rates in BP ($t = -0.53$, $P > 0.05$), FP ($t = -1.14$, $P > 0.05$), and SP neurons ($t = -1.4$, $P > 0.05$) showed no difference. Finally, a comparison of best rate of BP neurons also showed no difference ($t = -0.4484$, $P > 0.05$). These data indicate that the narrow range of rate selectivity observed in the C57 mouse cortex was unlikely to be influenced by early onset presbycusis.

FM direction selectivity. FM direction selectivity was studied in 90 neurons in A1 and AAF. Upward and downward sweeps with the same bandwidth were varied in duration to obtain FM rate selectivity functions. Direction selectivity was quantified using the direction selectivity index (DSI). Because

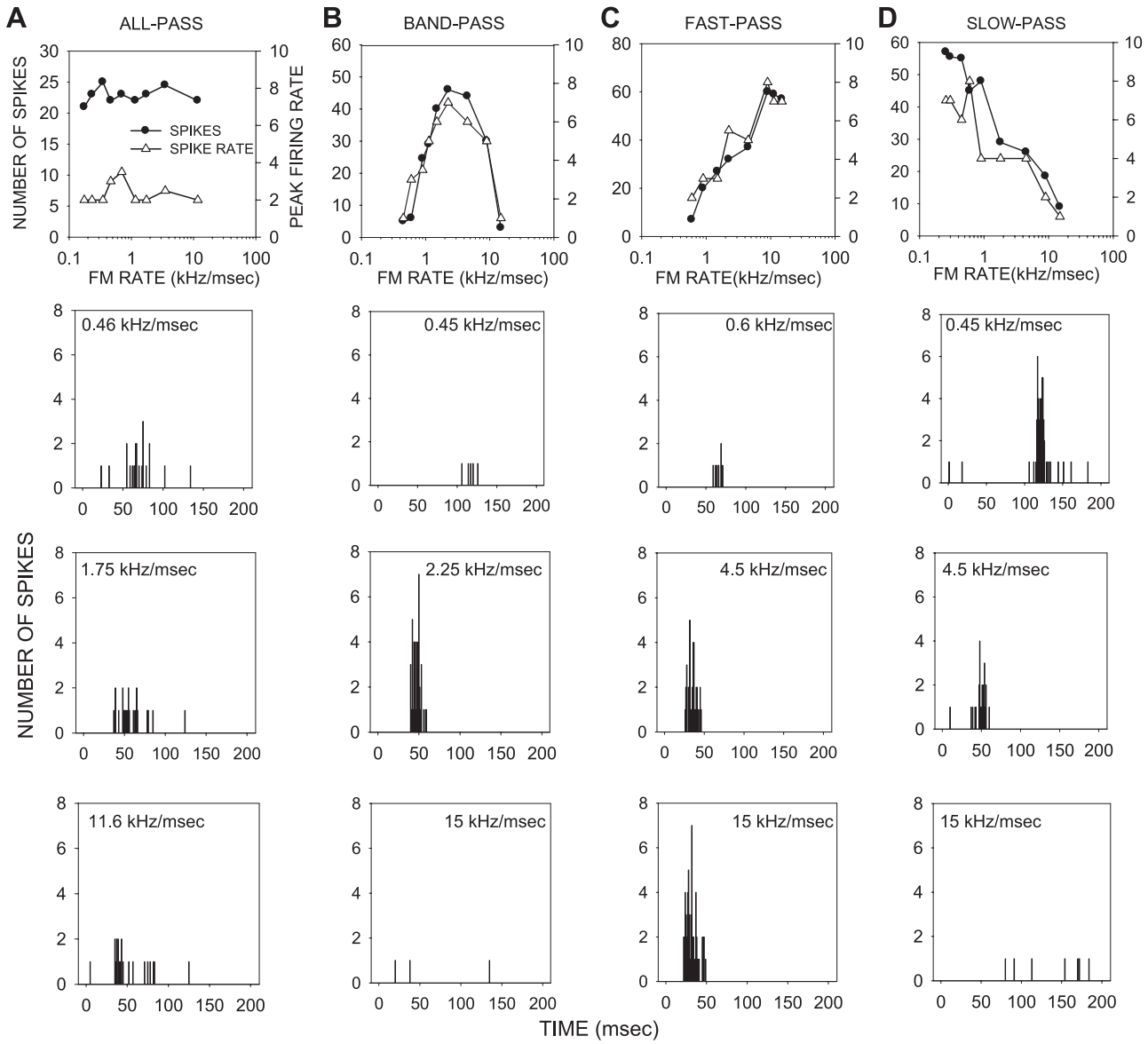

Fig. 2. Examples of FM rate selectivity functions (*A–D*) illustrate the rate selectivity type classification. Example poststimulus time histograms for each type of neuron are shown below each graph. *A*: all pass (AP). *B*: BP. *C*: FP. *D*: SP.

direction selectivity can vary with the sweep rate of the stimulus, DSI was measured at three different sweep rate ranges: 0.1–1, 1.1–3, and 3.1–10 kHz/ms.

Figure 4*A* shows an example of a direction-selective neuron that preferred downward sweeps. The DSI values at different sweep rate ranges are shown. Figure 4*B* shows a neuron that responded similarly to the two sweep directions. On average, there was very little direction selectivity in the mouse auditory cortex (Fig. 5). The average DSI was ~0 regardless of the sweep rate range (Fig. 5*A*). A one-way ANOVA of FM rate range × DSI revealed no effect of rate range [$F(2,269) = 1.13$, $P = 0.3234$]. Fewer than 20% of neurons showed a DSI value greater than 0.33 or less than −0.33 (twice the response to 1 direction compared with the other). There was no relationship between DSI and CF at any of the three sweep rates ($P > 0.05$, Fig. 5, *B–D*). Finally, in ~86% (77/90) of neurons, there was no difference in the FM rate selectivity type for upward and downward sweeps.

Effects of cortical depth on FM rate selectivity. The FM rate selectivity measures from single-unit recordings presented above were obtained at depths between 100 and 700 μm. A one-way ANOVA of FM tuning type × depth revealed a significant main effect of depth on FM tuning type [$F(3,197) = 3.57$, $P < 0.05$]. AP neurons were found deeper than BP and FP neurons (Fig. 6). This suggested a depth (cortical layer) effect on FM rate tuning.

To assess this directly, we measured FM rate properties at multiple depths in penetrations made orthogonal to the cortical surface. This was accomplished in 46 penetrations in both A1 and AAF. In each of these penetrations, FM rate selectivity was measured for a neuron isolated between 250 and 400 μm (mean depth 289 ± 63 μm) and compared with that for a neuron isolated deeper than 400 μm (mean depth 504 ± 91 μm). For the penetration shown in Fig. 7*A*, the neuron found at 356 μm was BP tuned. A second neuron isolated in the same penetration at 552 μm responded with greater number of spikes

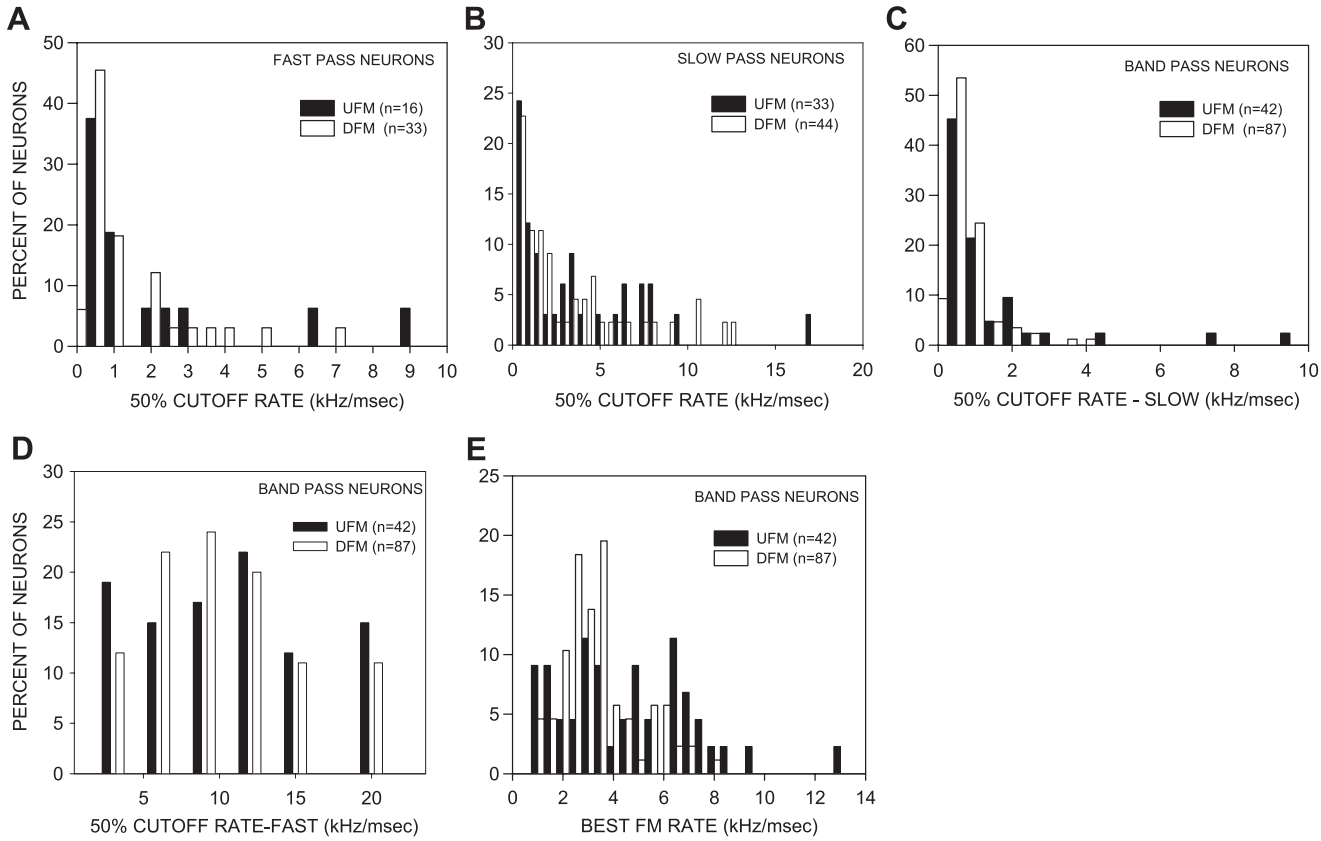

Fig. 3. *A*: distribution of 50% cutoff rate for FP neurons. These neurons respond at better than 50% of maximum response for rates faster than the cutoff. *B*: distribution of 50% cutoff rates for SP neurons. These neurons respond at better than 50% of maximum response at rates slower than the cutoff. *C* and *D*: BP neurons have two 50% cutoff rates, one as sweep rate is decreased (slow; *C*) and one as sweep rate is increased (fast; *D*). *E*: distribution of best rate in BP neurons. UFM, upward sweep. No significant differences were found between upward and downward sweep 50% cutoff rates.

and also responded similarly at all rates tested (AP). The neurons shown in Fig. 7*B* exhibited similar maximum responses, but the rate selectivity changed from BP to AP with depth. In 38/46 penetrations, rate selectivity changed type, with a BP-to-AP change occurring in 14 penetrations, a FP-to-AP change occurring in 7 penetrations, and a BP-to-FP change occurring in 7 penetrations. In 8/46 penetrations, there was no change in rate selectivity type with depth. The neurons shown in Fig. 7*C* exhibited similar rate selectivity functions independently of their depth. Across the population, a paired *t*-test revealed that neurons at shallow cortical depths had a significantly ($t = 5.8$, $P < 0.0001$) higher RTI value than more deeply located neurons (Fig. 7*D*). These results indicate FM rate selectivity decreases with cortical depth.

Table 1. *Mean (± s.e.m) rate tuning index (RTI) values for different types of neurons and for the two sweep directions. RTI is a unit-less measure*

Neurons	UFM	DFM
AP	0.24 ± 0.02	0.25 ± 0.01
BP	0.54 ± 0.02	0.5 ± 0.01
FP	0.51 ± 0.03	0.43 ± 0.02
SP	0.48 ± 0.02	0.45 ± 0.02

Values are means ± SE of rate tuning index (RTI) for different types of neurons and for the upward (UFM) and downward frequency-modulated (DFM) sweep directions. RTI is a unitless measure. AP, all pass; BP, band pass; FP, fast pass; SP, slow pass.

Multiunit mapping: A1 and AAF show different distributions of FM rate tuning types. Rate selectivity mapping studies were performed such that each penetration was ~100–200 μm from a neighboring penetration in the rostral/caudal and medial/lateral directions. Deviations from this were typically caused by vasculature in a given local area. For each penetration, a two-dimensional set of coordinates were determined using the scales on the Kopf electrode positioner, which were measured to the nearest 100 and 10 μm in the rostral/caudal and medial/lateral directions, respectively. The coordinates were then plotted using the Voronoi function in Matlab (Kilgard et al. 2001). Null points in which there were no penetrations were used around the borders to preserve the relative shape and area of the polygons. Because of the depth effects noted above, all mapping studies were done at depths between 250 and 450 μm. Only one recording was made per penetration in the mapping study. Single-unit and multiunit data show that within this depth range, rate selectivity type does not change significantly.

Figure 8 shows the CF and FM rate selectivity type maps (Voronoi tessellation; Kilgard et al. 2001) from five animals. Figure 8, *A–C*, shows maps in which both A1 and AAF were sampled. The number in each polygon indicates CF. The color of the polygon indicates FM rate selectivity type. The dashed contour line is the putative boundary between the two fields based on reversal in tonotopy (this was made by visual observation and not using any quantitative method). Figure 8, *D* and *E*, shows maps in which only the AAF was sampled as indicated by the decreasing tonotopy in the caudorostral direc-

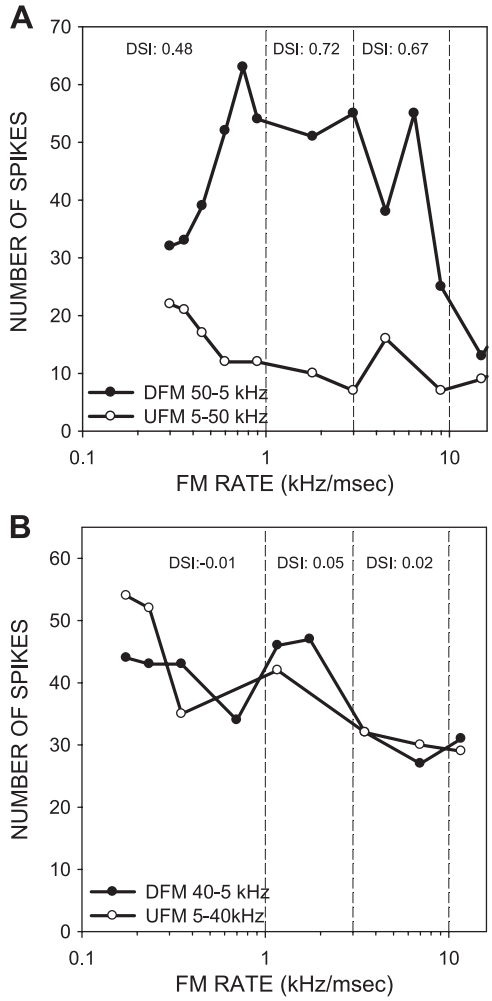

Fig. 4. FM direction selectivity in mouse auditory cortex. *A*: example of a direction-selective neuron. *B*: example of a nonselective neuron. DSI, direction-selective index.

tion (therefore, no dashed line). Caudal, rostral, and lateral boundaries were determined based on lack of responses to tones and sweeps. Medially, the boundary was determined based on responses typical of the dorsoposterior field (Stiebler et al. 1997) or based on lack of response. Therefore, the vast majority of the target areas, A1 and AAF, was sampled.

There was considerable interindividual variability in distribution of FM rate tuning type across A1/AAF, but two trends stood out. First, neurons with similar rate selectivity functions were clustered (Fig. 8). Clustering was quantified using a "neighbor analysis" wherein the percentage of sites with the same rate selectivity type was determined for each site. This was then compared with a neighbor analysis done on maps with the same x and y coordinates, but in which rate selectivity type was randomly assigned. For each randomly generated map, 10,000 iterations were performed. In the maps recorded from the mouse cortex, on average 53.6 ± 9.0% (mean ± SD) of neighbors were found to be of the same rate selectivity type for any given site. In the randomly generated maps, 25 ± 0.04% (mean ± SD) of neighbors were of the same type. These values were significantly different from each other ($t = 8.9$, $P < 0.0001$), indicating that neurons with similar rate selectivity types cluster together in A1 and AAF.

The second trend observed in the maps was that A1 comprised primarily SP neurons, with very few FP neurons. Across animals, AAF exhibited a more even distribution of FM rate selectivity types, with BP neurons forming the major class. Figure 9*A* quantifies the distribution of FM rate tuning types in A1 and AAF across all eight maps. There was a significant difference in the distributions with A1 dominated by SP neurons and BP neurons forming the major class in AAF ($\chi^2 = 31.7$, $P < 0.001$). Given that the precise boundary between AI and AAF cannot be delineated based on tonotopy alone, the analysis of distribution was also carried out after moving the boundary line to the right or left by one tessellation (e.g., by placing all neurons adjacent to the right of the dashed boundary lines in Fig. 8 in AI, or by placing all neurons adjacent to the left of the dashed boundary line in AAF). In either case, the distributions were statistically different (χ^2 test, $P < 0.001$), suggesting that the differences were not an artifact of the placement of the boundary line. Figure 9, *B* and *C*, shows that this distribution difference is not an artifact of oversampling a certain CF range in each area. Across the range of CFs, SP neurons dominate A1 and BP neurons form the major class in AAF. The distribution of FM rate tuning types does not depend on the CF range in A1 ($\chi^2 = 15.2$, $P = 0.1$). In the AAF, there is a trend for more FP neurons and less SP neurons with increasing CF range, but this is not statistically significant ($\chi^2 = 14.8$, $P = 0.1$). Together, these data illustrate that neurons in A1 and AAF cluster according to FM rate tuning types. Also, most neurons in A1 respond better to slow sweep rates, whereas neurons in AAF are selective for a narrow range of intermediate FM sweep rates or respond better to fast rates.

DISCUSSION

This study examined the cortical organization of FM sweep rate selectivity in the mouse. Three patterns of organization were discovered. First, there is a significant difference in the distribution of FM rate selectivity between A1 and AAF at recording depths between 250 and 450 μm. A1 neurons prefer slower rates than AAF neurons. Second, there are cortical depth-specific differences, with the dominant trend being a decline in FM rate selectivity with depth. Third, and perhaps the most striking finding, is the narrow range of FM rate selectivity exhibited by cortical neurons. Most of the BP neurons responded best to a narrow range of FM rates (~1–3 kHz/ms), and most FP and SP neurons exhibited 50% cutoff rates between 0.5 and 2 kHz/ms.

Comparison of FM rate selectivity across cortical areas and species. Neurons in mouse AAF show faster first spike and peak latencies, shorter receptive field durations (spectrotemporal receptive fields), and narrower spectral receptive fields than neurons in A1, suggesting more sensitivity to fast temporal modulation in AAF (Linden et al. 2003). The finding in the current study supports the hypothesis that AAF is specialized for faster temporal processing compared with A1. In the cat cortex as well, AAF is suggested to be more specialized for faster temporal processing (Imaizumi et al. 2004; Schreiner and Urbas 1988; Tian and Rauschecker 1994). The posterior auditory field of the cat appears to be more similar to A1, with mostly SP neurons and BP neurons selective for slow rates (Tian and Rauschecker 1998). These data suggest that across species, A1 and AAF are sensitive to different FM sweep rates.

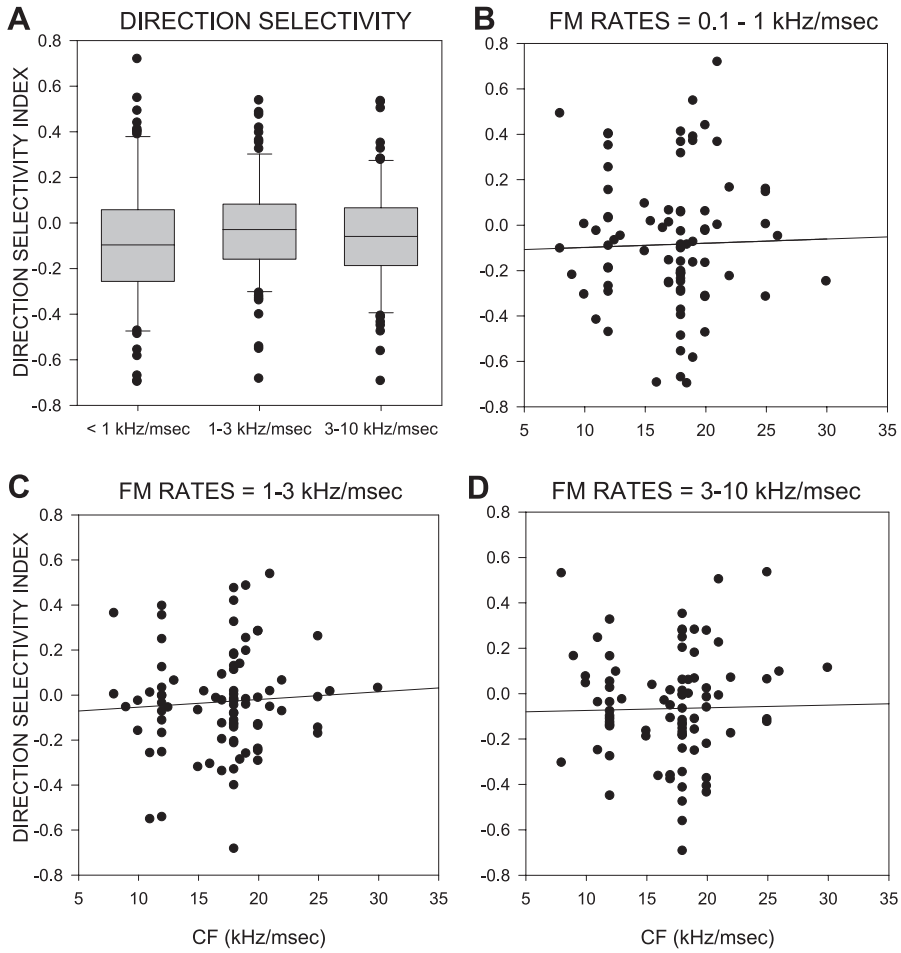

Fig. 5. *A*: distribution of DSI values measured at 3 different ranges of FM sweep rates. *B–D*: there was no correlation between characterization frequency (CF) and DSI at any of the 3 rate ranges tested. Positive DSI values indicate downward FM selectivity. Negative DSI values indicate upward sweep selectivity.

In the mouse, the depth-effect data indicate that the difference between A1 and AAF may be limited to depths between 250 and 450 μm, because most neurons located deeper than 450 μm exhibit reduced FM rate selectivity. In deeper layers, A1 and AAF may be more similar, with mostly nonselective or SP neurons. In the mouse cortex, depths between 250 and 450 μm correspond approximately to deep layer III and layer IV (granular layers; Anderson et al. 2009). Layers deeper than 450 μm correspond to infragranular layers. Both A1 and AAF receive inputs from the ventral division of the medial geniculate body (MGBv) (Lee and Winer 2011). Laminar analysis suggests A1 and AAF may be at the same hierarchical levels in auditory processing (Rouiller et al. 1991). Together, these data suggest that in the granular layers of auditory cortex, FM rate is processed in mostly segregated pathways, with slow rates driving A1 and intermediate and fast rates driving AAF. Whether the strong reciprocal connections between A1 and AAF (Lee and Winer 2011) play a role in shaping FM rate selectivity remains to be determined.

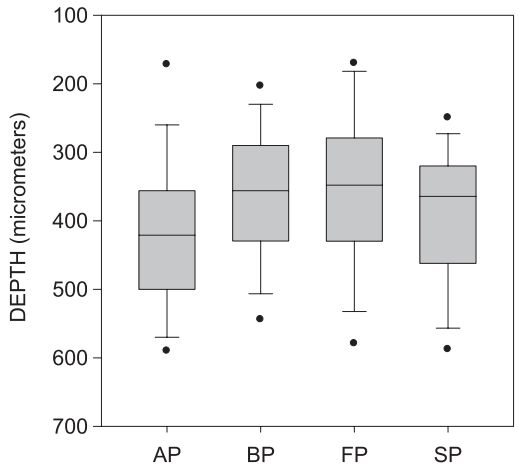

Fig. 6. Distribution of the depths at which neurons with different FM rate selectivity types were found across primary auditory cortex (A1) and the anterior auditory field (AAF) based on single-unit recordings. The boxes represent the 25th and 75th percentiles. The horizontal line within the boxes represents the median, and the vertical lines represent the standard deviation around the mean. The data points represent the 5th and 95th percentiles.

These data also suggest differences in how spectral and temporal properties of excitation and inhibition interact with each other in A1 and AAF. Studies of the pallid bat auditory cortex have shown that FM rate selectivity of the majority of BP and FP cortical neurons depends on interactions between excitatory receptive fields and sideband inhibition (Razak and Fuzessery 2006, 2008). Iontophoresis of $GABA_A$ receptor antagonists reduces or eliminates FM rate selectivity in ~50% of cortical neurons mainly by eliminating sideband inhibition or delaying inhibitory inputs (Razak and Fuzessery 2009). SP and AP neurons typically exhibit weak inhibitory sidebands, and their selectivity is not affected by $GABA_A$ receptor antagonists. This suggests that more neurons in AAF, compared with A1, exhibit stronger dependence on inhibitory sidebands in

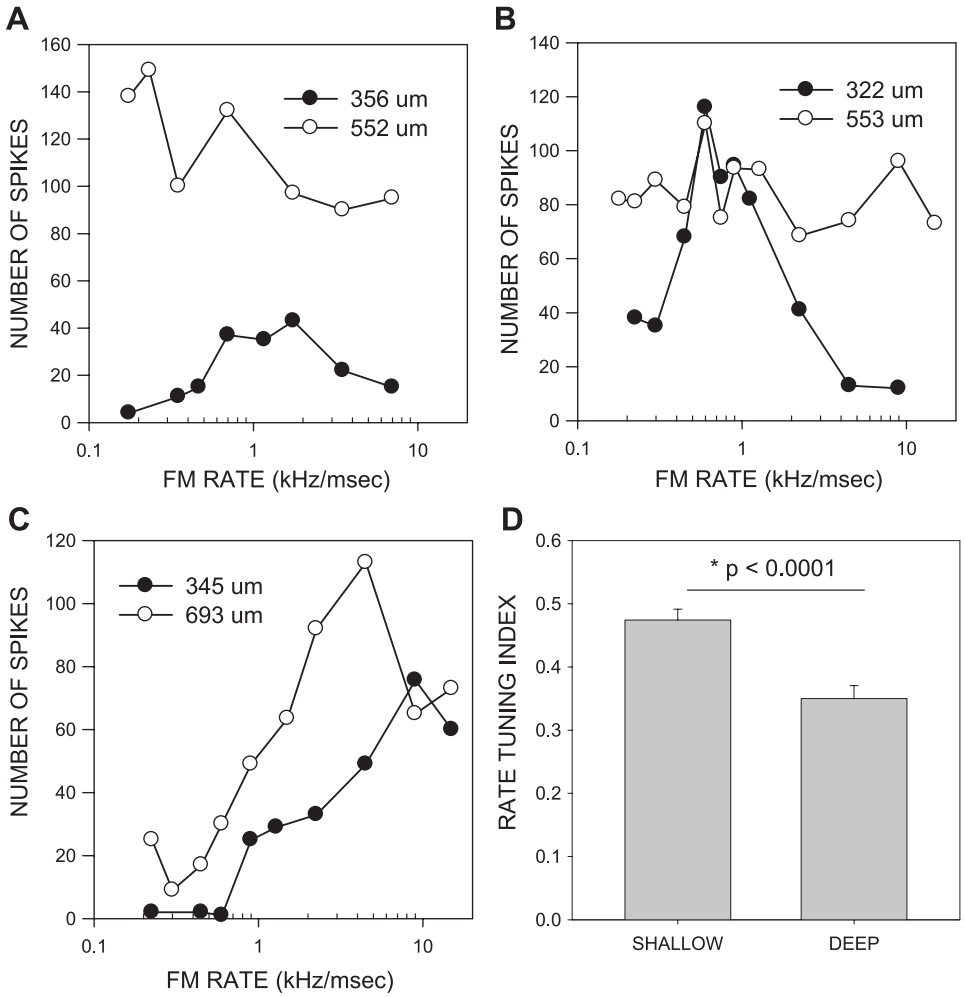

Fig. 7. *A–C*: representative FM rate selectivity functions from 2 different depths in orthogonal penetrations indicating depth-dependent changes in rate selectivity. *A*: a penetration in which response magnitude increased with depth and selectivity type changed from BP to AP. *B*: a penetration in which selectivity changed from BP to FP with depth without an increase in response magnitude. *C*: a penetration in which the rate selectivity type did not change with depth. *D*: rate tuning index (means ± SE) of neurons found in shallow vs. deeper layers in 28 penetrations.

shaping FM rate selectivity. The interactions between spike threshold and the magnitudes of inhibitory and excitatory conductance (Gittelman and Pollak 2011), which in turn can translate into timing differences, also may be different between A1 and AAF.

In the central nucleus of the inferior colliculus (ICc) of the mouse, a concentric organization of FM rate selectivity is present within isofrequency laminae (Hage and Ehret 2003) such that neurons sensitive to slower rates are present in the center and neurons sensitive to faster rates are present more peripherally (both laterally and medially in ICc). In auditory cortex of the mouse, a clustered organization of FM rate selectivity is present, with A1 dominated by neurons tuned to slow sweeps and AAF dominated by neurons tuned to fast or intermediate ranges of rates, regardless of CF. This suggests a reorganization of FM rate topography in the ascending auditory system (Portfors and Wenstrup 2001). Both A1 and AAF receive inputs from the ventral division of the MGBv of the thalamus, which in turn receives input from the ICc. It remains to be seen whether the central part of ICc connects (through MGB) to a larger extent to A1 than AAF, with more peripheral ICc inputs to AAF.

FM sweep direction selectivity. Fewer than 20% of neurons in the mouse A1 and AAF show DSI values greater than +0.3 or less than −0.3 at the FM sweep rate ranges tested. This is in contrast to that reported in the mouse inferior colliculus (IC), in which nearly one-half of the neurons exhibited direction selectivity according to the above criterion (Hage and Ehret 2003). Both studies used similar anesthetics (ketamine-xylazine), linear FM sweeps, and FM rates. The direction selectivity reported in the current study is also lower than that found in the auditory cortex of other species (44% in rats, Ricketts et al. 1998; 45% in cats, Mendelson et al. 1993). There was also no correlation between CF and DSI in our data set. Such correlations have been reported in rat and squirrel monkey A1 (Godey et al. 2005; Zhang et al. 2003) but not in the mouse IC (Hage and Ehret 2003) or owl monkey and cat A1 (Atencio et al. 2007; Heil et al. 1992; Mendelson et al. 1993). These differences are likely explained by the undersampling of neurons with CF <5 kHz and CF >30 kHz in our study. In the rat and squirrel monkey A1, high DSI values were typically found at the low or high end of the CF range sampled, particularly at frequencies near the beginning or the end of the fixed-bandwidth FM sweeps used to study sweep selectivity. A clearer picture of FM direction selectivity in the mouse cortex requires a broader sampling of CF range, but for regions of A1 and AAF with CF in the 7- to 30-kHz range, very little direction selectivity or correlation with CF is seen in the mouse. The implication of a lack of direction selectivity in most mouse cortical neurons studied presently is that the FM sweep rate selectivity and maps are likely to be similar for both sweep directions.

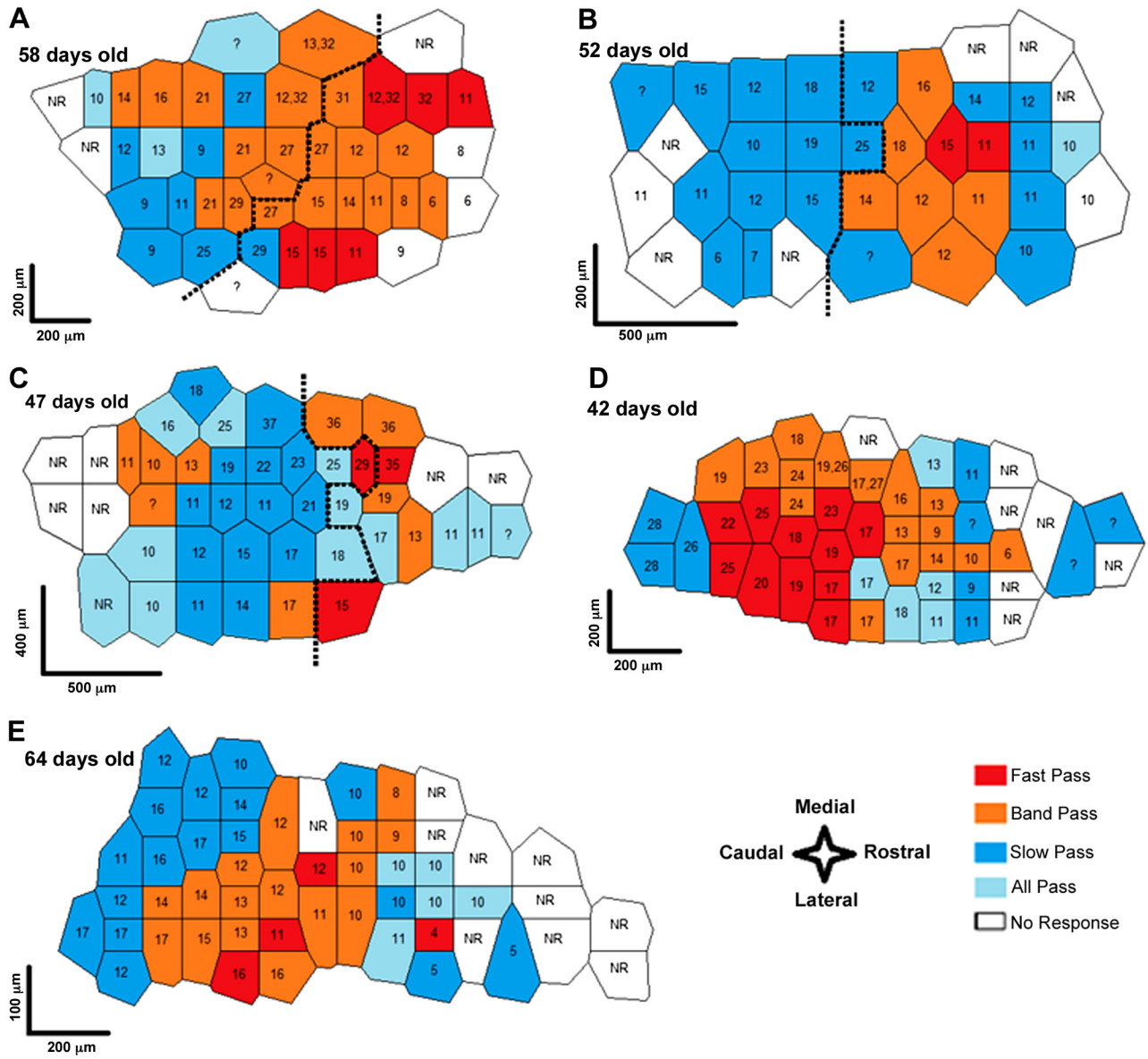

Fig. 8. FM sweep rate selectivity is differentially distributed across the auditory cortex. *A–E*: Voronoi tessellations of maps of FM rate selectivity (color of tessellation) and CF (number within each polygon) of multiunit recordings. Recordings were obtained at depths between 250 and 450 μm. The dotted line demarcates the putative boundary between A1 and AAF based on reversal in tonotopy. Only downward FM sweeps were used to determine FM rate selectivity in these maps.

Depth-dependent changes in FM rate selectivity. Cortical penetrations in which multiple neurons were isolated at different depths revealed a significant depth-dependent change in FM rate selectivity. FM rate tuning declined significantly with depth (250–400 vs. >450 μm), with the most prominent change being FP/BP to AP. These changes can occur with or without changes in maximal firing rates. The finding that FM rate selectivity declines from the granular to infragranular layers is consistent with findings in the cat A1, based on spectrotemporal receptive field analysis, that the infragranular layers are less feature selective and fire with less temporal precision than granular layers (Atencio et al. 2009). Thus, although properties such as CF and binaural interaction are similar at different depths (Abeles and Goldstein 1970; Imig and Adrian 1977), responses to dynamic stimuli may undergo significant changes across cortical layers. This may reflect differences in intracortical interactions shaping FM rate selectivity at different depths (Happel et al. 2010; Kaur et al. 2004). This may also reflect laminar differences in intrinsic properties in the mouse auditory cortex (Huggenberger et al. 2009).

Narrow range of response selectivity for FM rate in the mouse auditory cortex. For the range of FM rates tested in this study (0.08–20 kHz/ms), most SP and FP neurons had their 50% cutoff ~0.5–2 kHz/ms. The slow-rate cutoff of most BP neurons was also in the range of 0.5–2 kHz/ms. The 50% cutoff is approximately the center of FM rates across which the neuron shows maximum change in response magnitude. This range is therefore where maximum information is likely to be available (Harper and McAlpine 2004; Jazayeri and Movshon 2006). These data suggest that rates ~0.5–2 kHz/ms are best discriminated by the mouse auditory cortex. The majority of BP neurons in A1/AAF re-

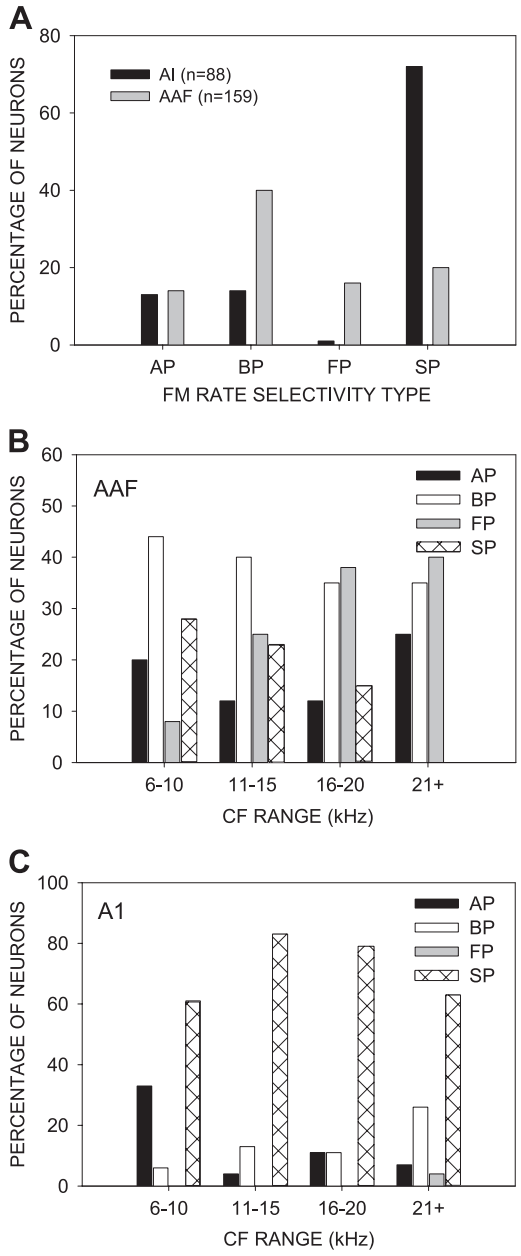

Fig. 9. *A*: distribution of FM rate selectivity types in A1 and AAF. The distribution of rate selectivity type is different between the 2 regions. *B*: distribution of rate selectivity types across CF ranges in AAF. *C*: distribution of rate selectivity types across CF ranges in A1.

sponded best to rates between 1 and 3 kHz/ms, indicating that BP neurons best detect this narrow range of rates. The best FM rates reported for the mouse are considerably faster than those reported in the owl and squirrel monkey A1 (Atencio et al. 2007; Godey et al. 2005). Although this may reflect species differences, it must be noted that we only report best rate for BP neurons. The monkey A1 studies report best rate (speed) for all classes of neurons. Thus, if SP neurons, which dominate A1 of the mouse, were included, the best rate would be much lower in the mouse cortex, as well. Likewise, the best rates reported presently are also faster than those reported in chinchilla A1 (Brown and Harrison 2009). However, in the chinchilla, only rates <1 kHz/ms were studied.

The functional significance of the selectivity for a narrow range of FM rates in the mouse auditory cortex is unclear. It is possible that these neurons discriminate sweep rates present in the rich repertoire of vocalizations emitted by mice. On the other hand, the narrow range of selectivity may reflect fundamental constraints on the mechanisms underlying FM rate selectivity. Most of these vocalizations have spectral energy in the range of 60–110 kHz (Grimsley et al. 2011; Holy and Guo 2005; Panksepp et al. 2007), whereas the neurons recorded presently had CF (and tuning) between 5 and 40 kHz. It has been suggested that neurons with this range of CF in the ICc indeed respond to very high-frequency vocalizations based on the distortion products with energy in the neurons' lower frequency tuning curve (Holmstrom et al. 2010; Portfors et al. 2009). This is true for both the tonal and FM components of vocalizations, which have different FM sweep rates. An examination of published sonograms of mouse vocalizations does indicate that there are a number of vocalizations with sweep rates between 0.5 and 2 kHz/ms (Grimsley et al. 2011; Liu et al. 2003; Portfors 2007). In C57 mice, three of the four dominant call types include FM sweeps (Panksepp et al. 2007). The FM rates of these sweeps are between 0.8 and 1.2 kHz/ms, which falls within the narrow range of cortical rate selectivity observed in this study. Thus the range of cortical rate selectivity may be relevant for processing vocalizations.

Neurons with CF extending into the 50- to 80-kHz range have been reported in the mouse cortex, in a region termed the ultrasonic field (UF; Stiebler et al. 1997). These neurons may play a role in processing vocalizations, as well. Given the differences in the distribution of FM rate selectivity between A1 and AAF, it is of interest to note that the UF connects strongly and reciprocally with ipsilateral A1 (with neurons with putative CFs between 20 and 40 kHz) but only weakly with AAF (Hofstetter and Ehret 1992). Thus neurons in UF and A1 may respond to calls with mostly tonal components (and slow rates), and neurons in the AAF may respond better to calls with rapid changes in frequencies. Both types of calls are present in mouse vocalizations (Grimsley et al. 2011; Panksepp et al. 2007).

Methodological considerations. The C57bl/6 strain of mouse was studied at ages <3 mo. This strain has been studied as a model for early onset presbycusis, and the data from this study serve as baseline for future work on how FM processing changes in presbycusis. However, the question arises whether the data shown in this study for young mice may be influenced by early onset hearing loss. Previous electrophysiological studies show that the C57 mice develop high-frequency loss from 3 to 6 mo (Henry and Chole 1980; Hunter and Willott 1987; Mikaelian 1979; Willott 1986) with a loss of outer hair cells in the basal 20% of the cochlea present from 3 mo of age (Spongr et al. 1997). Comparison of cochlear morphology, auditory brain stem responses, and distortion product otoacoustic emission responses shows that the C57 strain is similar to the CBA/CaJ strain at 1 mo and begins to deviate at 3 mo of age (Park et al. 2010). Auditory cortical responses and gross tonotopy appear to be normal in the young C57 mice (Bandyopadhyay et al. 2010) and start to show plasticity from 3 mo of age (Willot et al. 1993). Taberner and Liberman (2005) compared auditory nerve fiber responses between C57 (~4 mo) and CBA strains (age between 2 and 4 mo) and found no differences in spontaneous rates, tuning curves, rate vs. level

functions, dynamic range, response adaptation, phase-locking, and the relation between spontaneous rate and response properties. The only difference found in the 4-mo-old C57 mice was the expected elevation in high-frequency hearing at that age. Together, these studies show most changes in the C57 auditory system compared with that of the CBA strain begin to happen around 3 mo of age and become more pronounced between 3 and 6 mo. These studies also suggest that the 2-mo-old C57 mouse is comparable to the CBA strain. Our comparison of data from 1- to 2-mo-old and 2- to 3-mo-old cortex shows no significant differences in sweep rate selectivity measures. Thus we conclude that early onset presbycusis had minimal influence on the data and suggest that the narrow range of rate selectivity is likely to be typical of mouse cortex.

Conclusions. Speech recognition declines with aging and presbycusis. FM sweeps play an important role in speech processing (Zeng et al. 2005). Cortical FM sweep selectivity changes with age (Mendelson and Ricketts 2001). Thus FM rate selectivity may serve as a useful physiological probe to develop a model system in which contributions of both genetic and experience-dependent factors in auditory cortex aging and disease can be evaluated. The cortical mechanisms underlying FM sweep selectivity are known based on studies in bats and rodents (Razak and Fuzessery 2006; Ye et al. 2010). Preliminary data suggest similar mechanisms are operational in the mouse auditory cortex, as well. Ongoing studies address if and how cortical FM rate selectivity is altered by aging and presbycusis.

ACKNOWLEDGMENTS

We thank Dr. Don Gans for developing the hardware/software used in this study and Dr. Zoltan Fuzessery for providing useful comments on the manuscript.

GRANTS

This study was funded by a grant from the Deafness Research Foundation.

DISCLOSURES

No conflicts of interest, financial or otherwise, are declared by the authors.

REFERENCES

Abeles M, Goldstein MH. Functional architecture in cat primary auditory cortex: Columnar organization and organization according to depth. *J Neurophysiol* 33: 172–187, 1970.

Anderson LA, Christianson GB, Linden JF. Mouse auditory cortex differs from visual and somatosensory cortices in the laminar distribution of cytochrome oxidase and acetylcholinesterase. *Brain Res* 1252: 130–142, 2009.

Atencio CA, Blake DT, Strata F, Cheung SW, Merzenich MM, Schreiner CE. Frequency-modulation encoding in the primary auditory cortex of the awake owl monkey. *J Neurophysiol* 98: 2182–2195, 2007.

Atencio CA, Schreiner CE. Laminar diversity of dynamic sound processing in cat primary auditory cortex. *J Neurophysiol* 103: 192–205, 2010.

Atencio CA, Sharpee TO, Schreiner CE. Hierarchical computation in the canonical auditory cortical circuit. *Proc Natl Acad Sci USA* 106: 21894–21899, 2009.

Bandyopadhyay S, Shamma SA, Kanold PO. Dichotomy of functional organization in the mouse auditory cortex. *Nat Neurosci* 13: 361–368, 2010.

Brand A, Urban R, Grothe B. Duration tuning in the mouse auditory midbrain. *J Neurophysiol* 84: 1790–1799, 2000.

Brown T, Harrison RV. Responses of neurons in chinchilla auditory cortex to frequency-modulated tones. *J Neurophysiol* 101: 2017–2029, 2009.

Felsheim C, Ostwald J. Responses to exponential frequency modulations in the rat inferior colliculus. *Hear Res* 98: 137–151, 1996.

Fuzessery ZM, Richardson MD, Coburn MS. Neural mechanisms underlying selectivity for the rate and direction of frequency-modulated sweeps in the inferior colliculus of the pallid bat. *J Neurophysiol* 96: 1320–1336, 2006.

Gittelman JX, Pollak GD. It's about time: how input timing is used and not used to create emergent properties in the auditory system. *J Neurosci* 31: 2576–2583, 2011.

Gittelman JX, Li N, Pollak GD. Mechanisms underlying directional selectivity for frequency-modulated sweeps in the inferior colliculus revealed by in vivo whole-cell recordings. *J Neurosci* 29: 13030–13041, 2009.

Godey B, Atencio CA, Bonham BH, Schreiner CE, Cheung SW. Functional organization of squirrel monkey primary auditory cortex: responses to frequency-modulation sweeps. *J Neurophysiol* 94: 1299–1311, 2005.

Gordon M, O'Neill WE. Temporal processing across frequency channels by FM selective auditory neurons can account for FM rate selectivity. *Hear Res* 122: 97–108, 1998.

Gordon-Salant S, Fitzgibbons PJ. Sources of age-related recognition difficulty for time-compressed speech. *J Speech Lang Hear Res* 44: 709–719, 2001.

Grimsley JMS, Monaghan JJM, Wenstrup JJ. Development of social vocalizations in mice. *PLoS One* 6: e17460, 2011.

Hage SR, Ehret G. Mapping responses to frequency sweeps and tones in the inferior colliculus of house mice. *Eur J Neurosci* 18: 2301–2312, 2003.

Happel MF, Jeschke M, Ohl FW. Spectral integration in primary auditory cortex attributable to temporally precise convergence of thalamocortical and intracortical input. *J Neurosci* 30: 11114–11127, 2010.

Harper NS, McAlpine D. Optimal neural population coding of an auditory spatial cue. *Nature* 430: 682–686, 2004.

Heil P, Rajan R, Irvine DR. Sensitivity of neurons in cat primary auditory cortex to tones and frequency-modulated stimuli. I: Effects of variation of stimulus parameters. *Hear Res* 63: 108–134, 1992.

Henry KR, Chole RA. Genotypic differences in behavioral, physiological and anatomical expressions of age-related hearing loss in the laboratory mouse. *Audiology* 19: 369–383, 1980.

Hofstetter KM, Ehret G. The auditory cortex of the mouse: connections of the ultrasonic field. *J Comp Neurol* 323: 370–386, 1992.

Holmstrom LA, Eeuwes LB, Roberts PD, Portfors CV. Efficient encoding of vocalizations in the auditory midbrain. *J Neurosci* 30: 802–819, 2010.

Holy TE, Guo Z. Ultrasonic songs of male mice. *PLoS Biol* 3: e386, 2005.

Huggenberger S, Vater M, Deisz RA. Interlaminar differences of intrinsic properties of pyramidal neurons in the auditory cortex of mice. *Cereb Cortex* 19: 1008–1018, 2009.

Hunter KP, Willott JF. Aging and the auditory brainstem response in mice with severe or minimal presbycusis. *Hear Res* 30: 207–218, 1987.

Imaizumi K, Priebe NJ, Crum PC, Bedenbaugh PH, Cheung SW, Schreiner CE. Modular functional organization of cat anterior auditory field. *J Neurophysiol* 92: 444–457, 2004.

Imig TJ, Adrián HO. Binaural columns in the primary field (A1) of cat auditory cortex. *Brain Res* 138: 241–257, 1977.

Jazayeri M, Movshon JA. Optimal representation of sensory information by neural populations. *Nat Neurosci* 9: 690–696, 2006.

Kaur S, Lazar R, Metherate R. Intracortical pathways determine breadth of subthreshold frequency receptive fields in primary auditory cortex. *J Neurophysiol* 91: 2551–2567, 2004.

Kilgard MP, Pandya PK, Vazquez J, Gehi A, Schreiner CE, Merzenich MM. Sensory inputs directs spatial and temporal plasticity in primary auditory cortex. *J Neurophysiol* 86: 326–338, 2001.

Lee CC, Winer JA. Convergence of thalamic and cortical pathways in cat auditory cortex. *Hear Res* 274: 85–94, 2011.

Linden JF, Liu RC, Sahani M, Schreiner CE, Merzenich MM. Spectrotemporal structure of receptive fields in areas AI and AAF of mouse auditory cortex. *J Neurophysiol* 90: 2660–2675, 2003.

Liu RC, Miller KD, Merzenich MM, Schreiner CE. Acoustic variability and distinguishability among mouse ultrasound vocalizations. *J Acoust Soc Am* 114: 3412–3422, 2003.

Mendelson JR, Schreiner CE, Sutter ML, Grasse KL. Functional topography of cat primary auditory cortex: responses to frequency-modulated sweeps. *Exp Brain Res* 94: 65–87, 1993.

Mendelson JR, Ricketts C. Age-related temporal processing speed deterioration in auditory cortex. *Hear Res* 158: 84–94, 2001.

Merzenich MM, Jenkins WM, Johnston P, Schreiner C, Miller SL, Tallal P. Temporal processing deficits of language-learning impaired children ameliorated by training. *Science* 271: 77–81, 1996.

Mikaelian DO. Development and degeneration of hearing in the C57/b16 mouse: relation of electrophysiologic responses from the round window and cochlear nucleus to cochlear anatomy and behavioral responses. *Laryngoscope* 89: 1–15, 1979.

Nelken I, Versnel H. Responses to linear and logarithmic frequency-modulated sweeps in ferret primary auditory cortex. *Eur J Neurosci* 12: 549–562, 2000.

O'Neill WE, Brimijoin WO. Directional selectivity for FM sweeps in the suprageniculate nucleus of the mustached bat medial geniculate body. *J Neurophysiol* 88: 172–187, 2002.

Panksepp JB, Jochman KA, Kim JU, Koy JJ, Wilson ED, Chen Q, Wilson CR, Lahvis GP. Affiliative behavior, ultrasonic communication and social reward are influenced by genetic variation in adolescent mice. *PLoS One* 2: e351, 2007.

Park SN, Back SA, Park KH, Kim DK, Park SY, Oh JH, Park YS, Yeo SW. Comparison of cochlear morphology and apoptosis in mouse models of presbycusis. *Clin Exp Otorhinolaryngol* 3: 126–135, 2010.

Poon PWF, Chen X, Hwang JC. Basic determinants for FM responses in the inferior colliculus of rats. *Exp Brain Res* 83: 598–606, 1991.

Portfors CV. Types and functions of ultrasonic vocalizations in laboratory rats and mice. *J Am Assoc Lab Anim Sci* 46: 28–34, 2007.

Portfors CV, Roberts PD, Jonson K. Over-representation of species-specific vocalizations in the awake mouse inferior colliculus. *Neuroscience* 162: 486–500, 2009.

Portfors CV, Wenstrup JJ. Topographical distribution of delay-tuned responses in the mustached bat inferior colliculus. *Hear Res* 151: 95–105, 2001.

Razak KA, Fuzessery ZM. Facilitatory mechanisms underlying selectivity for the direction and rate of frequency modulated sweeps in the auditory cortex. *J Neurosci* 28: 9806–9816, 2008.

Razak KA, Fuzessery ZM. Neural mechanisms underlying selectivity for the rate and direction of frequency-modulated sweeps in the auditory cortex of the pallid bat. *J Neurophysiol* 96: 1303–1319, 2006.

Razak KA, Fuzessery ZM. GABA shapes selectivity for the rate and direction of frequency-modulated sweeps in the auditory cortex. *J Neurophysiol* 102: 1366–1378, 2009.

Ricketts C, Mendelson JR, Anand B, English R. Responses to time-varying stimuli in rat auditory cortex. *Hear Res* 123: 27–30, 1998.

Rouiller EM, Simm GM, Villa AE, de Ribaupierre Y, de Ribaupierre F. Auditory corticocortical interconnections in the cat: evidence for parallel and hierarchical arrangement of the auditory cortical areas. *Exp Brain Res* 86: 483–505, 1991.

Schreiner CE, Urbas JV. Representation of amplitude modulation in the auditory cortex of the cat. II. Comparison between cortical fields. *Hear Res* 32: 49–63, 1988.

Smith GE, Housen P, Yaffe K, Ruff R, Kennison RF, Mahncke HW, Zelinski EM. A cognitive training program based on principles of brain plasticity: results from the Improvement in Memory with Plasticity-based Adaptive Cognitive Training (IMPACT) Study. *J Am Geriatr Soc* 57: 594–603, 2009.

Spongr VP, Flood DG, Frisina RD, Salvi RJ. Quantitative measures of hair cell loss in CBA and C57BL/6 mice throughout their life spans. *J Acoust Soc Am* 101: 3546–3553, 1997.

Stevens KN, Klatt DH. Role of formant transitions in the voiced-voiceless distinction for stops. *J Acoust Soc Am* 55: 653–659, 1974.

Stiebler I, Neulist R, Fichtel I, Ehret G. The auditory cortex of the house mouse: left-right differences, tonotopic organization and quantitative analysis of frequency representation. *J Comp Physiol A* 181: 559–571, 1997.

Suga N. Analysis of frequency-modulated sounds by auditory neurones of echo-locating bats. *J Physiol* 179: 26–53, 1965.

Taberner AM, Liberman MC. Response properties of single auditory nerve fibers in the mouse. *J Neurophysiol* 93: 557–569, 2005.

Tallal P, Piercy M. Defects of non-verbal auditory perception in children with developmental aphasia. *Nature* 241: 468–469, 1973.

Tian B, Rauschecker JP. Processing of frequency-modulated sounds in the cat's anterior auditory field. *J Neurophysiol* 71: 1959–1975, 1994.

Tian B, Rauschecker JP. Processing of frequency-modulated sounds in the cat's posterior auditory field. *J Neurophysiol* 79: 2629–2642, 1998.

Tian B, Rauschecker JP. Processing of frequency-modulated sounds in the lateral auditory belt cortex of the rhesus monkey. *J Neurophysiol* 92: 2993–3013, 2004.

Washington SD, Kanwal JS. DSCF neurons within the primary auditory cortex of the mustached bat process frequency modulations present within social calls. *J Neurophysiol* 100: 3285–3304, 2008.

Willott JF. Effects of aging, hearing loss, and anatomical location on thresholds of inferior colliculus neurons in C57BL/6 and CBA mice. *J Neurophysiol* 56: 391–408, 1986.

Willott JF, Aitkin LM, McFadden SL. Plasticity of auditory cortex associated with sensorineural hearing loss in adult C57BL/6J mice. *J Comp Neurol* 329: 402–411, 1993.

Ye CQ, Poo MM, Dan Y, Zhang XH. Synaptic mechanisms of direction selectivity in primary auditory cortex. *J Neurosci* 30: 1861–1868, 2010.

Zeng FG, Nie K, Stickney GS, Kong YY, Vongphoe M, Bhargave A, Wei C, Cao K. Speech recognition with amplitude and frequency modulations. *Proc Natl Acad Sci USA* 102: 2293–2298, 2005.

Zhang LI, Tan AYY, Schreiner CE. Topography and synaptic shaping of direction selectivity in primary auditory cortex. *Nature* 424: 201–206, 2003.